A method for extracting coupled patterns of predictable and chaotic components in pairs of climate variables

C. S. Frederiksen[*]   X. Zheng[†]

(received 18 November 2004, revised 4 March 2005)

Abstract

Interannual variability in the seasonal mean of a climate variable can arise from a number of sources which can be categorized as (a) slowly varying (interannual/supra-annual) external forcing (for example, sea surface temperature forcing) and internal dynamics and (b) internal dynamics within the season. The former is generally assumed to be potentially predictable and the latter unpredictable. Here, a method is proposed for extracting coupled patterns of interannual variability that relate the predictable and unpredictable components in pairs of climate variables. The method is applied to observed Australian summer surface air temperature and the global 500 hPa geopotential height for the period 1951–1999.

---

[*]Bureau of Meteorology, GPO Box 1289K, Melbourne, Victoria, 3001, Australia. mailto:c.frederiksen@bom.gov.au

[†]National Institute of Water and Atmospheric Research, Wellington, New Zealand.

Contents

1 Introduction

The development of seasonal climate forecast schemes, whether statistical or dynamical, is predicated on an understanding of the sources of predictive skill as well as the sources of uncertainty in the variability of relevant climate variables. The seasonal mean of many climate variables can be thought of as consisting of two components [4, 6, 1, 7, 2, 3]; one is related to slowly varying boundary, or external, forcing on the climate system (for example, sea surface temperatures, sea-ice coverage and greenhouse gas concentration) and from slowly varying (interannual to supra-annual) internal atmospheric variability; the other is related to intraseasonal (month to month) variability. For the purposes of long-range (in advance of three months) forecasting, the former is generally considered as being potentially predictable, in that the forcing are themselves potentially predictable. The latter is related to meteorological phenomena that vary significantly within the season (for example, storms and atmospheric blocking, or intraseasonal variability associated with the Madden–Julian Oscillation) and is essentially unpredictable, or chaotic.

Important climate variables (the predictands), such as seasonal mean temperatures and seasonal mean rainfall, are largely related to local or hemispheric seasonal mean pressure fields (that is, the atmospheric circulation). Hence, a knowledge of the spatial patterns that relate the potentially predictable component of the seasonal mean pressure fields to that of the predictand should help us to understand the meteorological phenomena associated with forecast skill. Conversely, the identification of the spatial patterns that relate the intraseasonal component of the pressure field to that of the predictand should help us to understand the meteorological phenomena mainly responsible for the uncertainty in forecast skill, at the long range.

We propose a method for estimating the interannual cross-covariance matrices associated with the long range (in advance of a season) predictable and unpredictable components of a pair of climate variables. The method uses monthly mean time series of the climate variables. From the predictable and unpredictable cross-covariance matrices it is possible to construct coupled patterns of the predictable and chaotic components of covariability of the pair of climate variables. The method is applied to observed Australian summer (December–February, DJF) surface air temperature and the 500 hPa geopotential height, which is often used to characterize the global circulation.

2   Methodology

Let $t_{ym}(r)$ and $h_{ym}(s)$ represent monthly anomalies of two climate variables (for example, Australian surface air temperature and global 500 hPa geopotential height), in year y $(= 1, \ldots, Y)$, month m $(= 1, 2, 3)$ and at some location $r = 1, \ldots, R$ and $s = 1, \ldots, S$, not necessarily the same. Then, following [7], we assume

$$t_{ym}(r) = \bar{t}_y(r) + \tilde{t}_{ym}(r) \,, \tag{1}$$

$$h_{ym}(s) = \bar{h}_y(s) + \tilde{h}_{ym}(s) \,, \tag{2}$$

where $\bar{t}_y(r)$ and $\bar{h}_y(s)$ represent predictable components, which we refer to as the *slow* components, and $\tilde{t}_{ym}(r)$ and $\tilde{h}_{ym}(s)$ the intraseasonal component of each variable. The vectors $\mathbf{t}^T(r) = (\tilde{t}_{y1}(r), \tilde{t}_{y2}(r), \tilde{t}_{y3}(r))$ and $\mathbf{h}^T(s) = (\tilde{h}_{y1}(s), \tilde{h}_{y2}(s), \tilde{h}_{y3}(s))$ are assumed to comprise stationary and independent annual random vectors. The linear regression form (Eqns. (1) or (2)) implies that month-to-month fluctuations, or intraseasonal variability, arise entirely from this component (for example, $t_{y1}(r) - t_{y2}(r) = \tilde{t}_{y1}(r) - \tilde{t}_{y2}(r)$). We use the convention that an average over any index will be represented by a circle. Thus, for example, $t_{yo}(r)$ is an average over m months, and $t_{oo}(r)$ is an average over m months and Y years. The symbol V denotes the covariance of two variables.

Hence, the seasonal means of variables t and h is

$$t_{yo}(r) = \bar{t}_y(r) + \tilde{t}_{yo}(r), \tag{3}$$
$$h_{yo}(s) = \bar{h}_y(s) + \tilde{h}_{yo}(s), \tag{4}$$

where $\tilde{t}_{yo}(r)$ and $\tilde{h}_{yo}(s)$ are associated with intraseasonal variability, and $\bar{t}_y(r)$ and $\bar{h}_y(s)$ with the interannual variability of external forcing and slowly varying (interannual/supra-annual) internal dynamics.

An estimate of the covariance $V(\tilde{t}_{yo}(r), \tilde{h}_{yo}(s))$ using monthly means is made with the following assumptions. Since the daily time series of a climate variable, within a season, is in general assumed to be stationary, so are the monthly statistics. In particular, it follows that

$$V(\tilde{t}_{y1}(r), \tilde{h}_{y1}(s)) = V(\tilde{t}_{y2}(r), \tilde{h}_{y2}(s)) = V(\tilde{t}_{y3}(r), \tilde{h}_{y3}(s)). \tag{5}$$

The same is assumed to be true for the inter-monthly covariance, that is,

$$V(\tilde{t}_{y1}(r), \tilde{h}_{y2}(s)) = V(\tilde{t}_{y2}(r), \tilde{h}_{y3}(s)). \tag{6}$$

Finally, because daily weather events are unpredictable beyond a week or two, we assume that the intraseasonal components are uncorrelated if they are a month or more apart. That is,

$$V(\tilde{t}_{y1}(r), \tilde{h}_{y3}(s)) = 0. \tag{7}$$

Assumptions Eqns. (5–7) imply that,

$$E\left(\mathbf{t}(r)\mathbf{h}^T(s)\right) + E\left(\mathbf{h}(s)\mathbf{t}^T(r)\right) = 2\alpha \begin{pmatrix} 1 & \beta & 0 \\ \beta & 1 & \beta \\ 0 & \beta & 1 \end{pmatrix}, \tag{8}$$

where E denotes the expectation value based on all years and

$$\alpha = V(\tilde{t}_{ym}(r), \tilde{h}_{ym}(s)), \quad m = 1, 2, 3, \tag{9}$$

and

$$\begin{aligned}
\beta &= \frac{1}{2\alpha}[V(\tilde{t}_{y1}(r), \tilde{h}_{y2}(s)) + V(\tilde{h}_{y1}(s), \tilde{t}_{y2}(r))] \\
&= \frac{1}{2\alpha}[V(\tilde{t}_{y2}(r), \tilde{h}_{y3}(s)) + V(\tilde{h}_{y2}(s), \tilde{t}_{y3}(r))]. \tag{10}
\end{aligned}$$

In addition, using Eqns. (9–10),

$$\begin{aligned}
E &\left\{ \begin{pmatrix} \tilde{t}_{y1}(r) - \tilde{t}_{y2}(r) \\ \tilde{t}_{y2}(r) - \tilde{t}_{y3}(r) \end{pmatrix} \begin{pmatrix} \tilde{h}_{y1}(s) - \tilde{h}_{y2}(s) \\ \tilde{h}_{y2}(s) - \tilde{h}_{y3}(s) \end{pmatrix}^T \right\} \\
&+ E \left\{ \begin{pmatrix} \tilde{h}_{y1}(s) - \tilde{h}_{y2}(s) \\ \tilde{h}_{y2}(s) - \tilde{h}_{y3}(s) \end{pmatrix} \begin{pmatrix} \tilde{t}_{y1}(r) - \tilde{t}_{y2}(r) \\ \tilde{t}_{y2}(r) - \tilde{t}_{y3}(r) \end{pmatrix}^T \right\} \\
&= 2\alpha \begin{pmatrix} 2 - 2\beta & 2\beta - 1 \\ 2\beta - 1 & 2 - 2\beta \end{pmatrix}. \tag{11}
\end{aligned}$$

Since, from Eqn. (1), $t_{y1}(r) - t_{y2}(r) = \tilde{t}_{y1}(r) - \tilde{t}_{y2}(r)$ and $t_{y2}(r) - t_{y3}(r) = \tilde{t}_{y2}(r) - \tilde{t}_{y3}(r))$, with a similar relationship for h, the left hand side of Eqn. (11) can be evaluated using the given data $t_{ym}(r)$ and $h_{ym}(s)$. It follows then that

$$\alpha = a + b \quad \text{and} \quad \beta = \frac{a + 2b}{2(a + b)}, \tag{12}$$

where

$$a = \frac{1}{2}\left\{ \frac{1}{Y}\sum_{y=1}^{Y}[t_{y1}(r) - t_{y2}(r)][h_{y1}(s) - h_{y2}(s)] \right.$$

$$+ \frac{1}{Y} \sum_{y=1}^{Y} [t_{y2}(r) - t_{y3}(r)] [h_{y2}(s) - h_{y3}(s)] \Bigg\} , \tag{13}$$

$$b = \frac{1}{2} \Bigg\{ \frac{1}{Y} \sum_{y=1}^{Y} [t_{y1}(r) - t_{y2}(r)] [h_{y2}(s) - h_{y3}(s)]$$

$$+ \frac{1}{Y} \sum_{y=1}^{Y} [t_{y2}(r) - t_{y3}(r)] [h_{y1}(s) - h_{y2}(s)] \Bigg\} . \tag{14}$$

Using these estimates for α and β in Eqn. (8),

$$\frac{1}{2} [V(\tilde{t}_{y1}(r), \tilde{h}_{y2}(s)) + V(\tilde{h}_{y1}(s), \tilde{t}_{y2}(r))]$$

$$= \frac{1}{2} [V(\tilde{t}_{y2}(r), \tilde{h}_{y3}(s) + V(\tilde{h}_{y2}(s), \tilde{t}_{y3}(r))]$$

$$= \alpha\beta . \tag{15}$$

From Eqn. (7), it follows further that

$$V(\tilde{t}_{yo}(r), \tilde{h}_{yo}(s)) = \frac{1}{2} [V(\tilde{t}_{yo}(r), \tilde{h}_{yo}(s)) + V(\tilde{h}_{yo}(s), \tilde{t}_{yo}(r))]$$

$$= \frac{1}{18} \sum_{m,n=1}^{3} [V(\tilde{t}_{ym}(r), \tilde{h}_{yn}(s)) + V(\tilde{h}_{ym}(s), \tilde{t}_{yn}(r))]$$

$$= \frac{\alpha(3 + 4\beta)}{9} . \tag{16}$$

Following [7], we constrain β to lie within the interval $[0, 0.1]$ in order to reduce the estimation error. The covariance $V(t_{yo}(r), h_{yo}(s))$, which we shall refer to as the total covariance matrix, is estimated by the sample covariance,

$$V(t_{yo}(r), h_{yo}(s)) = \frac{1}{Y - 1} \sum_{y=1}^{Y} [t_{yo}(r) - t_{oo}(r)] [h_{yo}(s) - h_{oo}(s)] . \tag{17}$$

Thus, using Eqns (16) and (17), we define the residual covariance

$$
\begin{aligned}
&V(t_{yo}(r), h_{yo}(s)) - V(\tilde{t}_{yo}(r), \tilde{h}_{yo}(s) \\
={}&V(\bar{t}_y(r), \bar{h}_y(s)) + V(\bar{t}_y(r), \tilde{h}_{yo}(s)) + V(\bar{h}_y(s), \tilde{t}_{yo}(r)) \, . \qquad (18)
\end{aligned}
$$

In the case where the intraseasonal and slow components are independent, the residual covariance reduces to the covariance of the slow components only. Even when this is not the case, the coupled patterns associated with the residual covariance matrix can be shown to be more potentially predictable than those from the total covariance matrix, because the weather noise component has been largely removed. Eqns. (16–18) constructs the corresponding cross-covariance matrices from which the coupled spatial patterns are derived using a standard singular value decomposition (SVD) analysis [5, e.g.]. Associated with these patterns, one can derive time series showing how the sign of the patterns varies year by year. These time series are derived by projecting the original monthly data in each year onto each pattern [2, e.g.].

3   Example

Here, we apply our method to a study of Australian summer surface air temperature variability and its relationship to the global atmospheric circulation. The temperature data is taken from the Australian Bureau of Meteorology high quality surface temperature dataset interpolated onto a $2.5° \times 2.5°$ latitude/longitude grid. For the $500\,\mathrm{hPa}$ geopotential height we use the National Centers for Environmental Prediction (NCEP) and National Center for Atmospheric Research (NCAR) re-analysis data. This field effectively gives the height of the $500\,\mathrm{hPa}$ pressure level and is often used to study spatial patterns, or teleconnections, of interannual variability in the atmospheric circulation. The data is global and on a $5° \times 5°$ latitude/longitude grid. We consider the period 1951–1999.
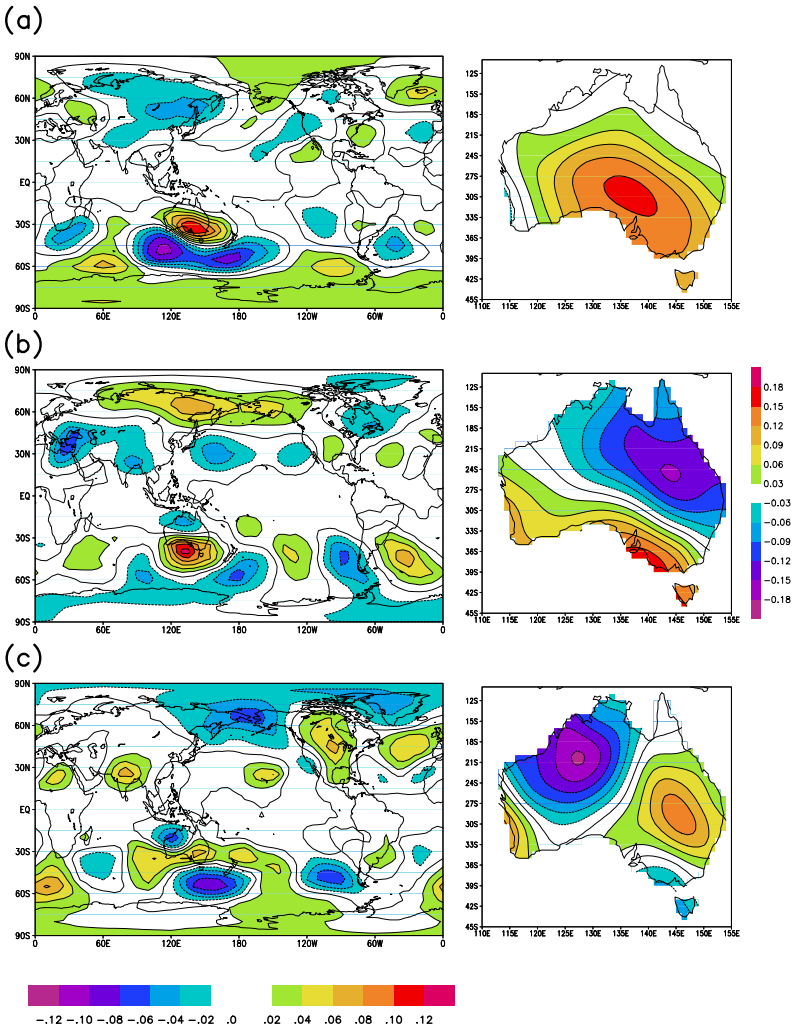
(a)

(b)

(c)

FIGURE 1: The first three dominant DJF coupled patterns of the intraseasonal components of Australian surface air temperature and global geopotential height covariability.

Figure 1 shows the first three dominant intraseasonal coupled patterns. They explain 24%, 16% and 10%, respectively, of the covariability in these fields. The first pattern (Figure 1(a)) depicts surface temperature variability over southern Australia associated with, at the particular phase shown, a dipole structure in the geopotential height field with positive (red shading) and negative (blue shading) height anomalies. The associated atmospheric winds go approximately anti-clockwise (clockwise) around the positive (negative) centre. Thus, at this phase, positive temperature anomalies are related to anticyclonic flow over southern Australia and cyclonic flow in the Australian Bight. This is a typical synoptic situation related to atmospheric blocking associated with intraseasonal internal dynamics.

The second pattern (Figure 1(b)), shows opposite temperature anomalies over northern and southern Australia associated with a meridional wave train of height anomalies extending from over northern Australia southward and then eastward into the Pacific Ocean. Again, at the phase shown, the negative (positive) temperature anomalies are consistent with the presence of cyclonic (anticyclonic) flow. Finally, pattern three (Figure 1(c)) is associated with a geopotential height wave train emanating from the northwest of Australia. These patterns represent the essentially unpredictable components of surface temperature and atmospheric height variability.

The two most important slow coupled patterns are shown in Figure 2. They explain 41% and 12%, respectively, of the covariability in the slow components. The variability is dominated by the first pattern (Figure 2(a)). In contrast to the intraseasonal patterns, where the geopotential height patterns show anomalies that are more localised in the Australian region, the slow geopotential height patterns have more global characteristics, usually indicative of some large scale forcing or slow internal dynamics. The most important forcing is generally sea surface temperature (SST). For the first pattern, positive temperature anomalies over central eastern Australia are related to positive geopotential height anomalies in a global band between 30°S to 30°N. There is also evidence of a Northern Hemisphere wave train (or

(a)

(b)

FIGURE 2: As in Figure 1, but for the first two slow components of coupled variability.
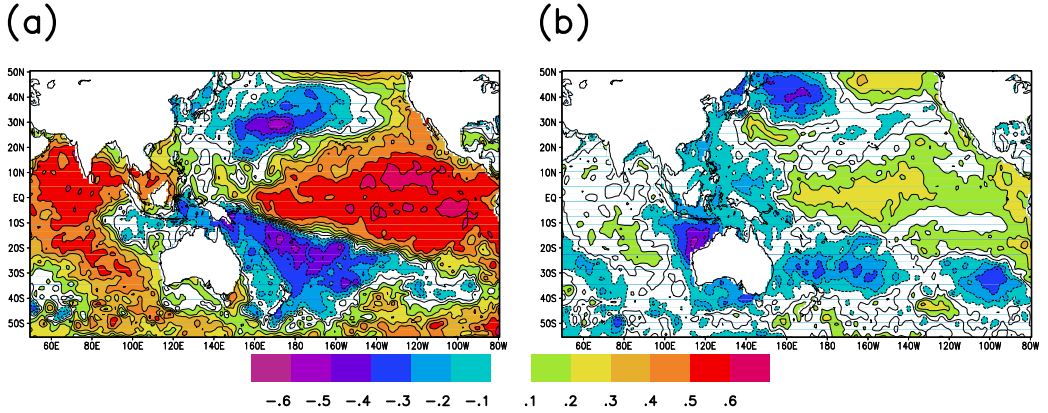
(a)

(b)
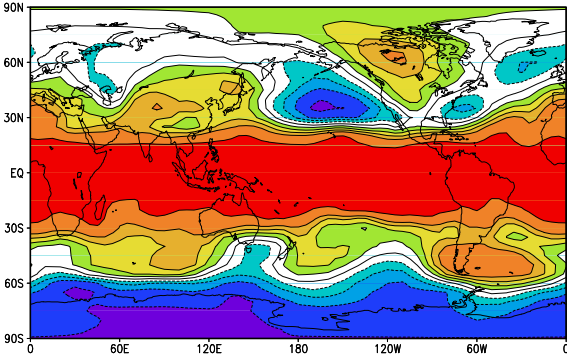
FIGURE 3: The correlation between observed sea surface temperature and the slow components of Australian surface temperature variability.

teleconnection). This atmospheric pattern is known to be associated with the El Nino–Southern Oscillation (ENSO) and sea surface temperature forcing in the tropical Pacific Ocean.

To illustrate this, we include correlations between the time series of our temperature patterns and corresponding time series of DJF SSTs. Here, we use the UK Meteorological Office Hadley Centre SST dataset. Figure 3(a) shows this correlation with this temperature pattern. There are clearly large correlations between eastern Australian temperature and SST anomalies in the tropical eastern Pacific. In particular, positive (negative) Australian temperature anomalies are associated with positive (negative) SST anomalies in the eastern Pacific.

The second coupled pattern (Figure 2(b)) shows positive temperature anomalies over the northwest and negative anomalies over the southeast of Australia, associated predominantly with geopotential height anomalies, of opposite sign, in the middle and high latitudes of the Southern Hemisphere. This height pattern has features of the Southern Annular Mode (SAM), an important teleconnection generally associated with slow internal dynamics.

Figure 3(b) shows that there is little large scale SST forcing of this coupled pattern.

4   Conclusions

We have proposed and examined a technique for extracting slow and intraseasonal coupled patterns of interannual variability from meteorological seasonal mean fields. The dominant intraseasonal patterns show consistent relationships between the temperature anomalies and geopotential height anomalies with positive (negative) temperature anomalies associated with anti-cyclonic (cyclonic) circulation. The intraseasonal height patterns are fairly localised, with largest weighting in the Australia region, and display features of Southern Hemisphere blocking and meridional wave trains, typically associated with internal dynamics at the intraseasonal time scale. The two most important slow patterns are related to ENSO and SAM, which are global scale atmospheric teleconnections. SST forcing plays an important role in the former, and slow internal dynamics in the latter.

A   Singular value decomposition

Here we provide a brief summary of the SVD analysis technique used to produce coupled spatial patterns of covariation from a given cross-covariance matrix. The interested reader is referred to [5] for more details.

Let $\mathbf{X}_{m \times t}$ and $\mathbf{Y}_{n \times t}$ be data matrices representing data from two climate variables at m and n geographical locations, respectively, and over t years. Assume further that the columns of the data matrices consists of deviations from the corresponding vector of sample means over all years. Without loss of generality, assume also that $m \leq n$. Then the cross-covariance matrix can

be written as

$$\mathbf{A}_{m\times n} = \frac{1}{t}\mathbf{X}_{m\times t}\mathbf{Y}_{n\times t}^{T}, \tag{19}$$

where $\mathbf{Y}_{n\times t}^{T}$ represents the transpose of $\mathbf{Y}_{n\times t}$. Any rectangular matrix can be given a singular value decomposition [5]

$$\mathbf{A}_{m\times n} = \mathbf{U}_{m\times n}\mathbf{D}_{n\times n}\mathbf{V}_{n\times n}^{T}, \tag{20}$$

where the columns of $\mathbf{U}$ and $\mathbf{V}$ are orthonormal vectors of dimension m and n and are called *left* and *right singular vectors*, respectively. Matrix $\mathbf{D}$ is a diagonal matrix with non-negative elements $d_{ii} = d_i$ for $i = 1,\ldots,n$, called *singular values*. Furthermore, the column vectors of $\mathbf{U}$ and $\mathbf{V}$ are the eigenvectors of the $\mathbf{A}\mathbf{A}^{T}$ and $\mathbf{A}^{T}\mathbf{A}$, respectively, with eigenvalues equal to the square of the singular values. For example,

$$\mathbf{A}\mathbf{A}^{T}\mathbf{U} = \mathbf{U}\mathbf{D}(\mathbf{V}^{T}\mathbf{V})\mathbf{D}^{T}(\mathbf{U}^{T}\mathbf{U}) = \mathbf{U}\mathbf{D}^{2}. \tag{21}$$

The pairs of singular vectors from $\mathbf{U}$ and $\mathbf{V}$, corresponding to the same singular value, are the coupled patterns we consider above.

References

[1] C. S. Frederiksen, A. P. Kariko and X. Zheng. A technique for extracting potentially predictable patterns from climate data. *ANZIAM J.*, 44(E):C160–C179, 2003. [Online] http://anziamj.austms.org.au/V44/CTAC2001/Fred. C277

[2] C. S. Frederiksen and X. Zheng. Variability of seasonal-mean fields arising from intraseasonal variability. Part 2, application to NH winter circulations. *Climate Dynamics*, 23:193–206, 2004. C277, C282

[3] C. S. Frederiksen and X. Zheng. A method for studying the influence of intra-seasonal variability on the inter-annual variability of climate

fields. *ANZIAM J.*, 45(E):C378–C390, 2004.
http://anziamj.austms.org.au/V45/CTAC2003/Fred C277

[4] R. A. Madden. Estimates of the natural variability of time averaged sea level pressure. *Mon. Wea. Rev.*, 104:942–952, 1976. C277

[5] H. von Storch and F. W. Zwiers. *Statistical Analysis in Climate Research.* Cambridge University Press, 484pp, 1999. C282, C287, C288

[6] X. Zheng and C. S. Frederiksen. Validating interannual variability in an ensemble of AGCM simulations. *J. Climate*, 12:2386–2396, 1999. C277

[7] X. Zheng and C. S. Frederiksen. Variability of seasonal-mean fields arising from intraseasonal variability. Part 1, methodology. *Climate Dynamics*, 23:177–191, 2004. C277, C278, C281